

Original Article

Distribution of pancreatic B cell imaging agent ^{99m}Tc -DTPA-NGN2 in the body and animal experimental research on pancreatic B cell functional imaging

Zhi-Hua Liu¹, Ying Xie¹, Jun Tang², Chun-Feng Liu³

Departments of ¹Endocrinology, ²Nuclear Medicine, ³Nurology, The Second Affiliated Hospital of Soochow University, Suzhou 215002, Jiangsu Province, China

Received January 15, 2016; Accepted February 17, 2016; Epub April 15, 2016; Published April 30, 2016

Abstract: Purpose: To explore the feasibility of the application of ^{99m}Tc -DTPA-Nateglinide as a nuclear medicine imaging agent for evaluating pancreatic B cell function. Methods: (1) Distribution of the experiment: Forty-two mice were selected and divided into seven groups. Each mice was injected with 3.7 MBq (100 μCi) of ^{99m}Tc -DTPA-NGN2 from the vena caudalis and was sacrificed by bloodletting at five minutes, 15 minutes, 30 minutes, one hour, two hours, four hours and six hours, respectively. Then, their tissues and organs such as the heart, liver, spleen, brain, kidneys, bones, small bowels, stomach and pancreas, and blood were collected, weighted, and their radioactivity was tested. Subsequently, the percentage injection dose rate (%ID/g) per gram of tissue was calculated. (2) Imaging experiment: Thirty-five mice were selected and divided into seven groups. Each was injected with 18.5 MBq (100 μCi) of ^{99m}Tc -DTPA-NGN2 from the vena caudalis and imaging were conducted at the same time as above. (3) Forty-eight Wistar rats were attained and randomly divided into four groups. The first group served as the healthy control group, while the second, third and fourth groups were diabetic model groups induced by intraperitoneally injecting STZ at different doses. Each group was injected with ^{99m}Tc -DTPA-Nateglinide from the vena caudalis, and radiological evaluations were conducted at 30 minutes, one hour, 1.5 hours and two hours, respectively. The data obtained were estimated using a correlation comparison with the levels of insulin and immunohistochemical count of beta cells. Results: The ^{99m}Tc -DTPA-Nateglinide demonstrated good imaging in the pancreases of mice and rats, and was positively correlated to the level of insulin and the number of pancreatic beta cells. Conclusion: Pancreatic beta cell imaging using ^{99m}Tc -DTPA-Nateglinide may be a method to evaluate pancreatic beta cell function.

Keywords: ^{99m}Tc -DTPA-Nateglinide, islet imaging, diabetes mellitus

Introduction

Diabetes is a metabolic disorder caused by an absolute or relative deficiency of insulin. Both type 1 and type 2 diabetes are characterized by deficits of beta cell: around 99% deficit in long-standing type 1 diabetes [1], and 65% deficit in long-standing type 2 diabetes [2]. Type 1 diabetes results from a selective destruction of the beta cells by a T-cell mediated autoimmune process [3]. Type 2 diabetes begins with insulin resistance in the peripheral tissues, a gradual increase in circulating blood glucose that triggers beta cells to release even more insulin, and subsequent failure of beta cells to maintain normal glucose homeostasis [4].

Currently, there is no ideal method for noninvasively measuring changes in functional β -cell

function, which would be valuable for assessing diabetes progression, following therapeutic response, or for evaluating the viability of transplanted pancreatic islets [5]. The goal in treating diabetes has turned from decreasing blood glucose to keeping and improving the function of pancreatic beta cells [6, 7].

However, the evaluation of pancreatic islets function is difficult with poor operation, and there are many contradictions and disputes. Noninvasive imaging techniques such as single photon emission computed tomography (SPECT) [8], positron emission tomography [9], bioluminescence imaging [10], and magnetic resonance imaging (MRI) [11-14] have shown promise in detecting BCM. However, these techniques have limitations. For example, β -cell mass can't reflect function exactly [6]. Moore A,

Distribution of pancreatic B cell imaging agent ^{99m}Tc -DTPA-NGN2

Bonner-Weir S, Weissleder R. Noninvasive in vivo measurement of beta-cell mass in mouse model of diabetes.

Nateglinide is a drug that clinically promotes the secretion of insulin from pancreatic B cells in patients with diabetes mellitus, and it can be bound to the sulfonylurea receptors of K_{ATP} on the membrane of pancreatic B cells and transported into cells [15], thereby promoting the release of insulin. In theory, nateglinide specifically combines with B cells that have insulin releasing function, making normal functioning B cells to image. However, apoptotic or failed B cells and other normal and pathological tissues of the pancreas could not be imaged; thus, the imaging of ^{99m}Tc -DTPA-Nateglinide can reflect the function of pancreatic islets.

^{99m}Tc -DTPA-NGN2 is one kind of nateglinide that uses DTPA as a chelating agent of labeling matter ^{99m}Tc . It was used as a nuclear medicine imaging agent for pancreatic imaging to evaluate the function of pancreatic islet beta cells and observe the comparability and correlation between imaging of ^{99m}Tc -DTPA-Nateglinide and other evaluations of the function of beta cells.

Materials and methods

Materials

The major reagent, DTPA-Nateglinide, was provided by the MD Anderson Cancer Center, University of Texas. The ^{99}Mo - ^{99m}Tc generator was purchased from Beijing Atom Hightech, Ltd. Mice and Wistar rats were purchased from the Experimental Animal Center of The Medical College of Soochow University. The immunohistochemical reagent was purchased from Wuhan Boster biotech, Ltd. Streptozotocin (STZ) was purchased from the SIGMA group. The blood glucose meter was provided by Johnson & Johnson (USA). The rat insulin detection kit was purchased from Shanghai Xitang.

Experimental methods

Labeling of DTPA-NGN2 and determination of the labeling rate: Stannous chloride and freshly rinsed $^{99m}\text{TcO}_4^-$ was added into the DTPA-NGN2 kit, which was shaken and left standing; thus, labeling was accomplished. Labeling rate was determined by paper chromatography,

the expansion agent was a mixed solution of ammonium acetate and methanol at a 4:1 ratio of 1 mol/L. Agents of 95% labeling rate and above can be used in the experiment.

Experiment on the distribution in normal mice body: Forty-two normal mice were attained and divided into seven groups, with six mice in each group. Each was injected with 3.7 MBq (100 μCi) of ^{99m}Tc -DTPA-NGN2 from the vena caudalis, and was sacrificed by bloodletting at five minutes, 15 minutes, 30 minutes, one hour, two hours, four hours and six hours, respectively; thus, their tissues and organs such as the heart, liver, spleen, brain, kidneys, bones, small bowels, stomach, pancreases and blood were collected, weighted, and their radioactivity was tested. Then, the percentage injection dose rate (%ID/g) per gram of tissue was calculated.

Imaging experiment in normal mice: Five normal mice were injected with 3.7 MBq (100 μCi) of ^{99m}Tc -DTPA-NGN2 from the vena caudalis, and were sacrificed at five minutes, 15 minutes, 30 minutes, one hour, two hours, four hours and six hours, respectively. Thereafter, tissues and organs were attained and imaging was conducted. The imaging instrument was the coincidence single photon emission computed tomography (SPECT) from PICKER DHC, with a pinhole collimator.

Examination on diabetic rats: Forty-eight eight-week-old normal male Wistar rats were obtained and randomly assigned into four groups, with 12 rats in each group. The first group served as the normal control group, while the second and third or fourth groups served as the diabetic model groups. Fasting blood glucose (fasting for 12 hours) and random blood glucose were detected in all rats. In the present study, random blood glucose was defined as blood glucose in the non-fasting state. A 0.4% STZ solution was prepared using a citric acid-sodium citrate buffer (0.1 mmol/L, pH 4.2) and was used to fast all rats for 12 hours. Thereafter, the second, third and fourth groups of rats were intraperitoneally injected with STZ at body weight doses of 45 mg/kg, 55 mg/kg and 70 mg/kg, respectively. The first group of rats was only injected with the corresponding citric acid buffer. After one week, random blood glucose in rats in the STZ injection group were detected, with the inclusion criteri-

Distribution of pancreatic B cell imaging agent ^{99m}Tc-DTPA-NGN2

Table 1. Biological distribution of ^{99m}Tc-DTPA-NGN2 in normal mice (%ID/g)

	5 min	15 min	30 min	1 h	2 h	4 h	6 h
Heart	1.47±0.19	0.67±0.11	0.39±0.04	0.29±0.05	0.19±0.07	0.19±0.02	0.17±0.03
Liver	1.58±0.21	0.89±0.12	0.90±0.35	0.75±0.14	0.51±0.09	0.38±0.08	0.41±0.05
The spleen	1.18±0.13	0.53±0.13	0.56±0.14	0.42±0.14	0.32±0.04	0.33±0.09	0.29±0.03
Lung	2.96±0.50	1.43±0.24	0.69±0.18	0.73±0.05	0.67±0.24	0.45±0.12	0.48±0.23
Brain	0.21±0.03	0.13±0.03	0.19±0.04	0.17±0.02	0.08±0.03	0.16±0.05	0.12±0.05
Renal	12.67±4.42	5.18±0.86	3.85±0.49	2.79±0.50	2.01±0.29	1.48±0.27	1.56±0.23
Muscle	1.04±0.18	0.56±0.09	0.40±0.14	0.28±0.10	0.19±0.08	0.23±0.10	0.15±0.06
Bone	1.14±0.31	0.70±0.11	0.79±0.19	0.76±0.26	0.73±0.20	0.54±0.21	0.60±0.22
Sausage	1.45±0.19	0.78±0.24	1.05±0.50	0.93±0.38	0.86±0.29	0.27±0.06	0.40±0.06
Stomach	1.61±0.27	0.76±0.09	0.64±0.18	0.61±0.26	0.44±0.20	0.32±0.09	0.34±0.11
Pancreas	0.88±0.22	0.59±0.13	0.86±0.15	1.11±0.09	1.56±0.08	1.02±0.06	0.74±0.08
Blood	6.17±0.86	2.95±0.23	1.57±0.10	1.00±0.10	0.61±0.13	0.59±0.17	0.55±0.08

The data in the table for: $\bar{x} \pm s$.

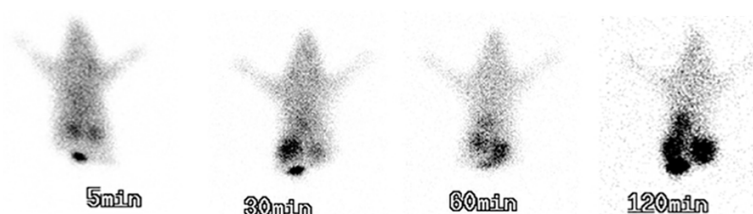


Figure 1. Imaging in pancreas became gradually clear over time. In 1-2 hours, pancreatic tissues could be clearly observed.

on of a DM model, in which random blood glucose was more than or equal to 11.1 mmol/L continuously for three days; and rats that did not meet this requirements were removed. On the tenth day, 2 ml of blood was collected from the orbit of each rat, and serum was separated to detect the level of insulin. Then, each rat was injected with 3.7 MBq (100 μ Ci) of ^{99m}Tc-DTPA-Nateglinide from the vena caudalis, and was sacrificed after 30 minutes. Rats were dissected, and part of the liver was taken for nuclear medicine determination. The tails of the pancreas were grouped into two: one group was for nuclear medicine determination; and the other group was placed in 10% neutral buffered formalin and fixed in preparation for light microscopic examination and immunohistochemistry. Five immunohistochemical slices were randomly selected, beta cell numbers were counted under high power microscopic view, and their average value was attained. Two diabetic mice were randomly selected and injected with 18.5 MBq (100 μ Ci) of ^{99m}Tc-DTPA-NGN2 from the vena caudalis. Then, they were sacrificed at five minutes, 15 minutes, 30 minutes, one hour, two hours, four hours and six hours, respectively. Thereafter, tissues and organs

were collected and imaging was conducted.

Data collation and analysis

All data were analyzed by SPSS 11.0 software, and variables were presented as ($\bar{x} \pm SD$). Variance analysis and *t*-test were used to compare differences between groups.

Correlations between factors were analyzed by Pearson's related analysis. *P*<0.05 was considered statistically significant.

Results

The distribution of ^{99m}Tc-DTPA-NGN2 in normal mice is shown in **Table 1**

The %ID/g data of tissues and organs revealed that the kidney was the main metabolic pathway of ^{99m}Tc-DTPA-NGN2, the brain did not absorb radioactivity, the muscle also absorbed less, the %ID/g of each organ decreased rapidly within one hour after injection, and the %ID/g of the pancreas gradually increased over time; and this was maintained at a high level in 1-2 hours. Imaging results (**Figure 1**) were consistent with the results of biological distribution experiments, imaging in pancreas became gradually clear with time, and pancreatic tissues could be clearly observed in 1-2 hours.

Histological observation of rat pancreatic islets

In H&E staining under a light microscope, the number of islets was greater in the normal

Distribution of pancreatic B cell imaging agent ^{99m}Tc -DTPA-NGN2

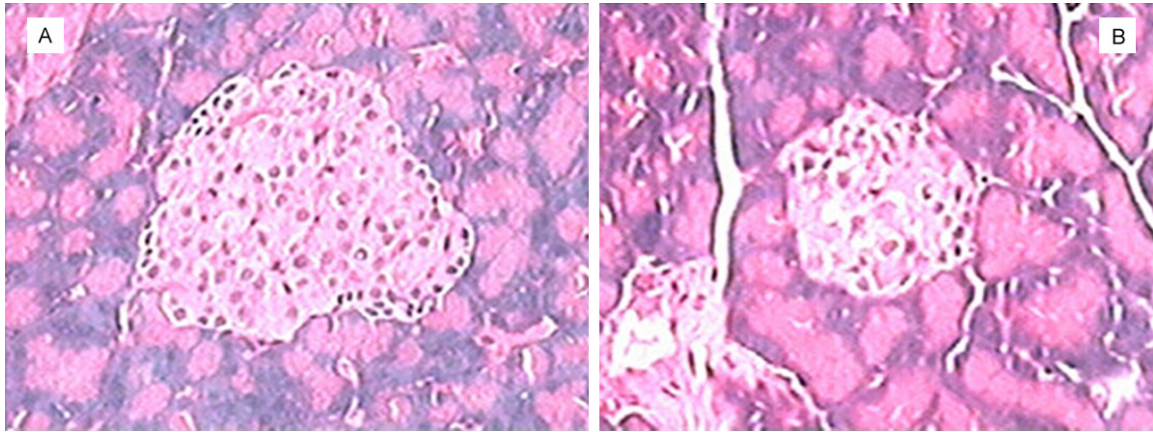


Figure 2. HE staining under light microscope observation of normal and diabetic rat islets. A: H&E stained pancreatic islets in rats in the normal group; B: H&E stained pancreatic islets in rats in the diabetic group.

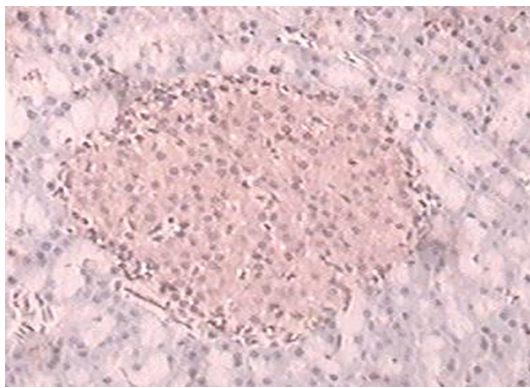


Figure 3. Immunohistochemical staining of rats in the normal group is shown, and the insulin expression of B cells was positive.

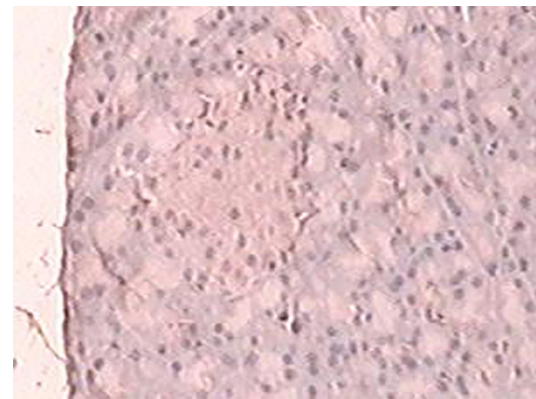


Figure 5. Pancreatic islets of immunohistochemical staining in rats in the diabetic group are shown. The number of B cells diminished and insulin expression was negative.

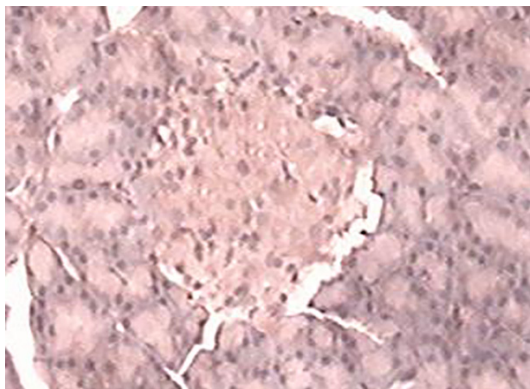


Figure 4. Pancreatic islets of immunohistochemical staining in rats in the diabetic group are shown, and the insulin expression of B cells was weak-positive.

group, the islets were bigger and clear, and the boundaries were distinct. Small and flat cells were surrounding the islets, bigger and round

cells were located in the middle, the nucleus had a uniform size, and cytoplasm was plump (**Figure 2A**). In each group of diabetic rats, there were different degrees of damage to the pancreatic islets; that is, the number of islet cells decreased and diameters of the pancreatic islets diminished. Some of the islets disintegrated and underwent necrosis, vacuole-like matters were presented in the middle, and the nuclei were not clear; thus, the characteristics of cell necrosis was obvious (**Figure 2B**).

Under immunohistochemical staining, islets in rats in the normal group were stained more obviously than the surrounding tissues, the nuclei of β cells was clear, and the cytoplasm was stained homogeneously (**Figure 3**). The islets of diabetic rats were stained unevenly, with little difference between the surrounding

Distribution of pancreatic B cell imaging agent ^{99m}Tc -DTPA-NGN2

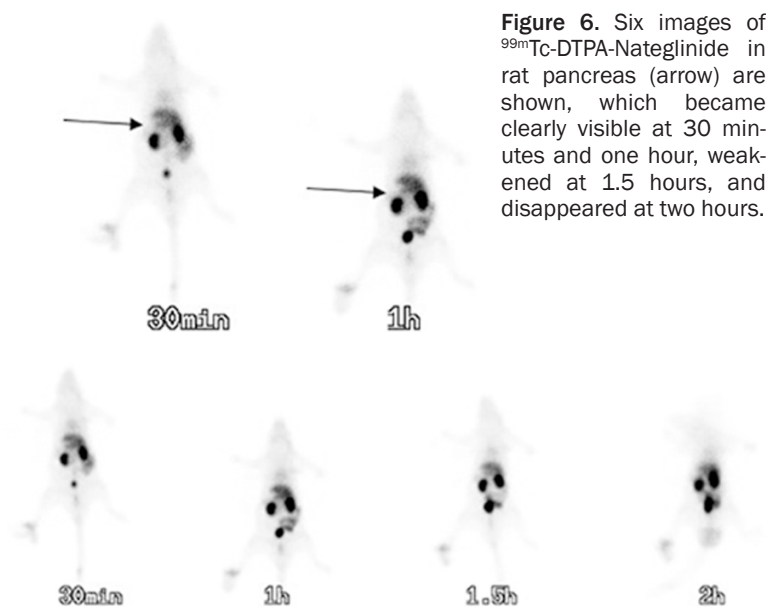


Figure 6. Six images of ^{99m}Tc -DTPA-Nateglinide in rat pancreas (arrow) are shown, which became clearly visible at 30 minutes and one hour, weakened at 1.5 hours, and disappeared at two hours.

tissues. The boundaries were not distinct, the diameters of the islets decreased, the number of stained cells was reduced, and vacuoles were presented locally (**Figures 4 and 5**).

*Imaging of ^{99m}Tc -DTPA-Nateglinide in rat pancreas was good (**Figure 6**), and imaging ratio of the pancreas to the liver in different dose groups of rats were significantly different ($P < 0.05$, **Tables 2 and 3**)*

It can be observed that as the dose of STZ increased, β cell count decreased, and damage to pancreatic islet beta cells was aggravated. Following the decrease in insulin level, imaging ratio of the pancreas to the liver diminished. Imaging ratio of the pancreas to the liver detected by ^{99m}Tc -DTPA-Nateglinide in different dose groups was positively correlated with insulin level and the number of β cells (**Figure 3**).

Discussion

In the diagnosis and treatment effect evaluation of diabetes, accurate quantification of beta cells is the key challenge to understanding the loss and dysfunction of beta cells in the course of diabetes [16]. At present, methods for detecting the function of pancreatic islet beta cells are mainly the stimulation of glucose, the insulin secretion stimulated by non-glucose matters, and the secretion function of other substances [17]. Among them, the hyperglycemic clamp technique has been considered as

the standard method for evaluating pancreatic cell function, and the sensitivities of other tests arranged from high to low: intravenous glucose stimulation test, tolbutamide stimulation test, arginine stimulation test, glucagon stimulation test and oral glucose tolerance test (OGTT) [18]. The hyperglycemic clamp technique suffers from a complex operation, and is expensive and time-consuming; thus, it is difficult to be widely popularized in clinic [19]. Intravenous glucose tolerance test (IVGTT) is performed by injecting a 50% glucose solution in 1-3 minutes, and blood is taken at

the relevant time in three hours after injection (a total of 23 times) [20]. Compared with the hyperglycemic clamp, it is relatively simple and has good repeatability; but it is also more cumbersome, fever, flushing and other side effects may occur, and blood sampling times may also bring physical pain to patients.

Thus, clinically, the evaluation of the insulin secretion function of beta cells is only a "rough" qualitative analysis. Physicians can only evaluate the function of beta cells in patients with the degree of disease progression, blood glucose and insulin levels, and response to therapy; which has brought lags in diagnosis and treatment [21]. In order to find an objective, simple, noninvasive and inexpensive method to evaluate the function of pancreatic islet cells, ^{99m}Tc -DTPA-Nateglinide was used as a nuclear medicine imaging agent to determine the function of pancreatic islet beta cells, and the comparability and correlation between ^{99m}Tc -DTPA-Nateglinide imaging and other evaluation methods was observed.

David Yang and Tony Yu, fellows of the MD Anderson Cancer Center, University of Texas, have long been working on the research and development of nuclear medicine imaging agents; and they have successfully developed ^{99m}Tc -DTPA-Nateglinide as a radionuclide imaging agent for pancreatic and neuroendocrine tumors; that is, DTPA serves as a bridge between ^{99m}Tc and Nateglinide-NGN2, combin-

Distribution of pancreatic B cell imaging agent ^{99m}Tc-DTPA-NGN2

Table 2. The fasting blood glucose, radiological imaging of pancreas to liver ratio, serum insulin levels, and beta cell count in each group of rats ($\bar{x} \pm SD$)

Group	Case	Fasting blood glucose (mmol/L)	Pancreatic and liver ratio	Serum insulin	β Cell count (/HP)
1	12	5.11 \pm 0.45	0.73 \pm 0.20	676.0 \pm 229.1	64.5 \pm 12.73
2	10	13.55 \pm 1.92*,#	0.47 \pm 0.25*	448.0 \pm 198.3*	40.5 \pm 21.83*
3	10	14.23 \pm 2.70*,#	0.37 \pm 0.12*,#	320.5 \pm 197.43*,#	26.5 \pm 11.04*,#
4	12	14.90 \pm 3.90*,#	0.33 \pm 0.11*,#	189.0 \pm 134.17*,#	24.0 \pm 12.94*,#

Note: *compare with 1 P<0.05, #compare with 1 P<0.01.

Table 3. Correlation analysis on data of the radiological imaging of pancreas to liver ratio, serum insulin levels, and beta cell count (r value)

	Pancreatic and liver ratio	Serum insulin	β cell count
Pancreatic and liver ratio		0.716*	0.790*
Insulin level			0.639*

Note: *P<0.01.

ing ^{99m}Tc and NGN2 at both ends of the DTPA. Thus, this gives rise to DTPA-NGN2 (ethylene dicysteine-deoxy glucose) labeled with ^{99m}Tc. As DTPA-NGN2 is labeled with ^{99m}Tc, it can be clearly imaged on the gamma camera and SPECT. In the process of detecting small lesions of pancreatic and neuroendocrine tumors, it was found that it can reflect the extent of damage of pancreatic islet B cells.

In this study, we found that the %ID/g of each organ rapidly decreased one hour after injection; while the %ID/g of the pancreas gradually increased with time, which was kept at a higher level in 1-2 hours. Imaging results were consistent with the results of biological distribution experiments, imaging in the pancreas became gradually clear with time, and pancreatic tissues could be clearly observed in two hours. This result indicates that it may be a good B cell imaging agent, and it is worthy of further study in the application of functional imaging of pancreatic B cells and pancreatic tumor imaging.

The dose of nateglinide in the treatment was three times per day, 60-120 mg per time. When the dose reached as high as 720 mg for seven days in a clinical trial, no obvious adverse reaction occurred [22]. When it was used for imaging, the dose was only 1 mg/70 kg, far below the clinical dose used to stimulate insulin secretion. Furthermore, it does not cause hypoglycemia and has better safety; hence, imaging

cost is considerably lower than that of the glucose clamp.

The occurrence of diabetes in rats induced by STZ was dose-dependent [23]. We peritoneally injected different doses of STZ in rats and hoped to observe

different degrees of pancreatic beta cell destruction. Results revealed that: ^{99m}Tc-DTPA-Nateglinide has good imaging in normal rat pancreas, while imaging has gradually decreased with the increase in damage of pancreatic islet function. At the same time, the level of serum insulin also decreased. The radiological imaging ratio of the pancreas to the liver was positively correlated with the beta cell count.

Furthermore, this correlation was more obvious than that between the serum insulin level and beta cell count, which indicate that it has a bright future in clinical application [24].

Diabetes induced by STZ in rats was similar to that of type I. In the future, we would apply this new method to animal models of diabetes type II and explore the correlation between radiological imaging and function of pancreatic islet beta cells in case of insulin resistance.

Acknowledgements

Thanks to the University of Texas M. Anderson cancer center, David Yang and D. Tony Yu DTPA-NGN2 kit.

Address correspondence to: Chun-Feng Liu, Department of Neurology, The Second Hospital of Suzhou University, No.1055 of Sanxiang Road, Suzhou 215002, Jiangsu Province, China. Tel: +86 051267784179; Fax: +86 0512-67784176; E-mail: chunfengliudoc@163.com

References

- [1] Meier JJ, Bhushan A, Butler AE, Rizza RA, Butler PC. Sustained beta cell apoptosis in patients with long-standing type 1 diabetes: indirect evidence for islet regeneration? *Diabetologia* 2005; 48(11): 2221-2228.
- [2] Butler AE, Janson J, Bonner-Weir S, Ritzel R, Rizza RA, Butler PC. Beta-cell deficit and in-

Distribution of pancreatic B cell imaging agent ^{99m}Tc-DTPA-NGN2

- creased beta-cell apoptosis in humans with type 2 diabetes. *Diabetes* 2003; 521: 102-110.
- [3] Palmer JP, Fleming GA, Greenbaum CJ, Herold KC, Jansa LD, Kolb H, Lachin JM, Polonsky KS, Pozzilli P, Skyler JS, Steffes MW. C-peptide is the appropriate outcome measure for type 1 diabetes clinical trials to preserve beta-cell function: report of an ADA workshop, 21-22 October 2001. *Diabetes* 2004; 531: 250-264.
- [4] Dwarakanathan A. Diabetes update. *J Insur Med* 2006; 3820-30.
- [5] Antkowiak PF, Stevens BK, Nunemaker CS, McDuffie M, Epstein FH. Manganese-Enhanced Magnetic Resonance Imaging Detects Declining Pancreatic β -Cell Mass in a Cyclophosphamide-Accelerated Mouse Model of Type 1 Diabetes. *Diabetes* 2013; 62: 44-48.
- [6] Jung KY, Kim KM, Lim S. Therapeutic Approaches for Preserving or Restoring Pancreatic β -Cell Function and Mass. *Diabetes Metab J* 2014; 38: 426-36.
- [7] Ludvigsson J. Therapies to Preserve β -Cell Function in Type 1 Diabetes. *Drugs* 2016; 76: 169-85.
- [8] Simpson NR, Souza F, Witkowski P, Maffei A, Raffo A, Herron A, Kilbourn M, Jurewicz A, Herold K, Liu E, Hardy MA, Van Heertum R, Harris PE. Visualizing pancreatic beta-cell mass with [¹¹C]DTBZ. *Nucl Med Biol* 2006; 33: 855-864.
- [9] Souza F, Simpson N, Raffo A, Saxena C, Maffei A, Hardy M, Kilbourn M, Goland R, Leibel R, Mann JJ, Van Heertum R, Harris PE. Longitudinal noninvasive PET-based beta cell mass estimates in a spontaneous diabetes rat model. *J Clin Invest* 2006; 116: 1506-1513.
- [10] Yong J, Rasooly J, Dang H, Lu Y, Middleton B, Zhang Z, Hon L, Namavari M, Stout DB, Atkinson MA, Tian J, Gambhir SS, Kaufman DL. Multimodality imaging of β -cells in mouse models of type 1 and 2 diabetes. *Diabetes* 2011; 60: 1383-1392.
- [11] Gimi B, Leoni L, Oberholzer J, Braun M, Avila J, Wang Y, Desai T, Philipson LH, Magin RL, Roman BB. Functional MR microimaging of pancreatic beta-cell activation. *Cell Transplant* 2006; 15: 195-203.
- [12] Antkowiak PF, Tersey SA, Carter JD, Vandsburger MH, Nadler JL, Epstein FH, Mirmira RG. Noninvasive assessment of pancreatic beta-cell function in vivo with manganese-enhanced magnetic resonance imaging. *Am J Physiol Endocrinol Metab* 2009; 296: E573-E578.
- [13] Antkowiak PF, Vandsburger MH, Epstein FH. Quantitative pancreatic beta cell MRI using manganese-enhanced Look-Locker imaging and two-site water exchange analysis. *Magn Reson Med* 2012; 67: 1730-1739.
- [14] Lamprianou S, Immonen R, Nabuurs C, Gjinovci A, Vinet L, Montet XC, Gruetter R, Meda P. High-resolution magnetic resonance imaging quantitatively detects individual pancreatic islets. *Diabetes* 2011; 60: 2853-2860.
- [15] Chen M, Hu C, Jia W. Pharmacogenomics of glinides. *Pharmacogenomics* 2015; 16: 45-60.
- [16] Tiedge M. Inside the pancreas: progress and challenges of human beta cell mass quantification. *Diabetologia* 2014; 57: 856-859.
- [17] He Y, Wang C, Li F, Gheng H, Yan L. Comparison of non-glucose versus glucose stimulation test in estimating islet β -cell function in individuals with differential glucose tolerance. [Article in Chinese] *Zhonghua Yi Xue Za Zhi* 2013; 93: 760-763.
- [18] Zhu M, Jia MP. Evaluation method of pancreatic B cell function and the clinical significance. *Foreign Medical Sciences, Endocrinology Volume* 2002, 22: 211-214.
- [19] Donga E, Dekkers OM, Corssmit EP, Romijn JA. Insulin resistance in patients with type 1 diabetes assessed by glucose clamp studies: systematic review and meta-analysis. *Eur J Endocrinol* 2015; 173: 101-109.
- [20] Kim DL, Kim SD, Kim SK, Park S, Song KH. Is an Oral Glucose Tolerance Test Still Valid for Diagnosing Diabetes Mellitus? *Diabetes Metab J* 2015.
- [21] Hou X, Liu J, Song J, Wang C, Liang K, Sun Y, Ma Z, Yang W, Li C, Zhang X, Lin P, Gong L, Wang M, Liu F, Li W, Yan F, Qin J, Wang L, Liu J, Zhao R, Chen S, Chen L. Relationship of Hemoglobin A1c with β Cell Function and Insulin Resistance in Newly Diagnosed and Drug Naive Type 2 Diabetes Patients. *J Diabetes Res* 2016; 2016: 8797316.
- [22] Zhou J, Deng Z, Lu J, Li H, Zhang X, Peng Y, Mo Y, Bao Y, Jia W. Differential therapeutic effects of nateglinide and acarbose on fasting and postprandial lipid profiles: a randomized trial. *Diabetes Technol Ther* 2015; 17: 229-234.
- [23] Szkudelski T. Streptozotocin-nicotinamide-induced diabetes in the rat. Characteristics of the experimental model. *Exp Biol Med (Maywood)* 2012; 237: 481-490.
- [24] Laurent D, Vinet L, Lamprianou S, Daval M, Filhoulaud G, Ktorza A, Wang H, Sewing S, Juretschke HP, Glombik H, Meda P, Boisgard R, Nguyen DL, Stasiuk GJ, Long NJ, Montet X, Hecht P, Kramer W, Rutter GA, Hecksher-Sørensen J. Pancreatic β -cell imaging in man: fiction or option? *Diabetes Obes Metab* 2016; 18: 6-15.